Supplementary materials

Linchao Li[1,2], Bin Wang[1,2*], Puyu Feng[3], Jonas Jägermeyr[4,5,6], Senthold Asseng[7], Christoph Müller[6], Ian Macadam[8], De Li Liu[2,9,*], Cathy Waters[10], Yajie Zhang[1], Qinsi He[11], Yu Shi[1], Shang Chen[12], Xiaowei Guo[13], Yi Li[14], Jianqiang He[14], Hao Feng[2,14], Guijun Yang[15], Hanqin Tian[16], Qiang Yu[1*]

[1] State Key Laboratory of Soil Erosion and Dryland Farming on the Loess Plateau, College of Natural Resources and Environment, Northwest A&F University, Yangling 712100, China

[2] NSW Department of Primary Industries, Wagga Wagga Agricultural Institute, Wagga Wagga, NSW 2650, Australia

[3] College of Land Science and Technology, China Agricultural University, Beijing 100193, China

[4] NASA Goddard Institute for Space Studies, New York, NY, USA

[5] Columbia University, Center for Climate Systems Research, New York, NY, USA

[6] Potsdam Institute for Climate Impacts Research (PIK), Member of the Leibniz Association, Potsdam, Germany

[7] Technical University of Munich, School of Life Sciences, Freising, Germany

[8] CSIRO Climate Innovation Hub, Australia

[9] Climate Change Research Centre, University of New South Wales, Sydney, NSW 2052, Australia

[10] NSW Department of Primary Industries, Dubbo NSW 2830, Australia

[11] School of Life Sciences, Faculty of Science, University of Technology Sydney, PO Box 123, Broadway, NSW 2007, Australia

[12] Key Laboratory of Meteorological Disaster, Ministry of Education and Collaborative Innovation Center on Forecast and Evaluation of Meteorological Disasters, Nanjing University of Information Science and Technology, Jiangsu Province, Nanjing 210044, China

[13] Key Laboratory of Adaptation and Evolution of Plateau Biota, Northwest Institute of Plateau Biology, Chinese Academy of Sciences, Xining, China

[14] College of Water Resources and Architectural Engineering, Northwest A&F University, Yangling, 712100, China

[15] Key Laboratory of Quantitative Remote Sensing in Agriculture of Ministry of Agriculture and Rural Affairs, Information Technology Research Center, Beijing Academy of Agriculture and Forestry Sciences, Beijing, 100097, China

[16] Schiller Institute for Integrated Science and Society, Department of Earth and Environmental Sciences, Boston College, Chestnut Hill, MA 02467, USA

* Correspondence: bin.a.wang@dpi.nsw.gov.au; de.li.liu@dpi.nsw.gov.au; yuq@nwafu.edu.cn

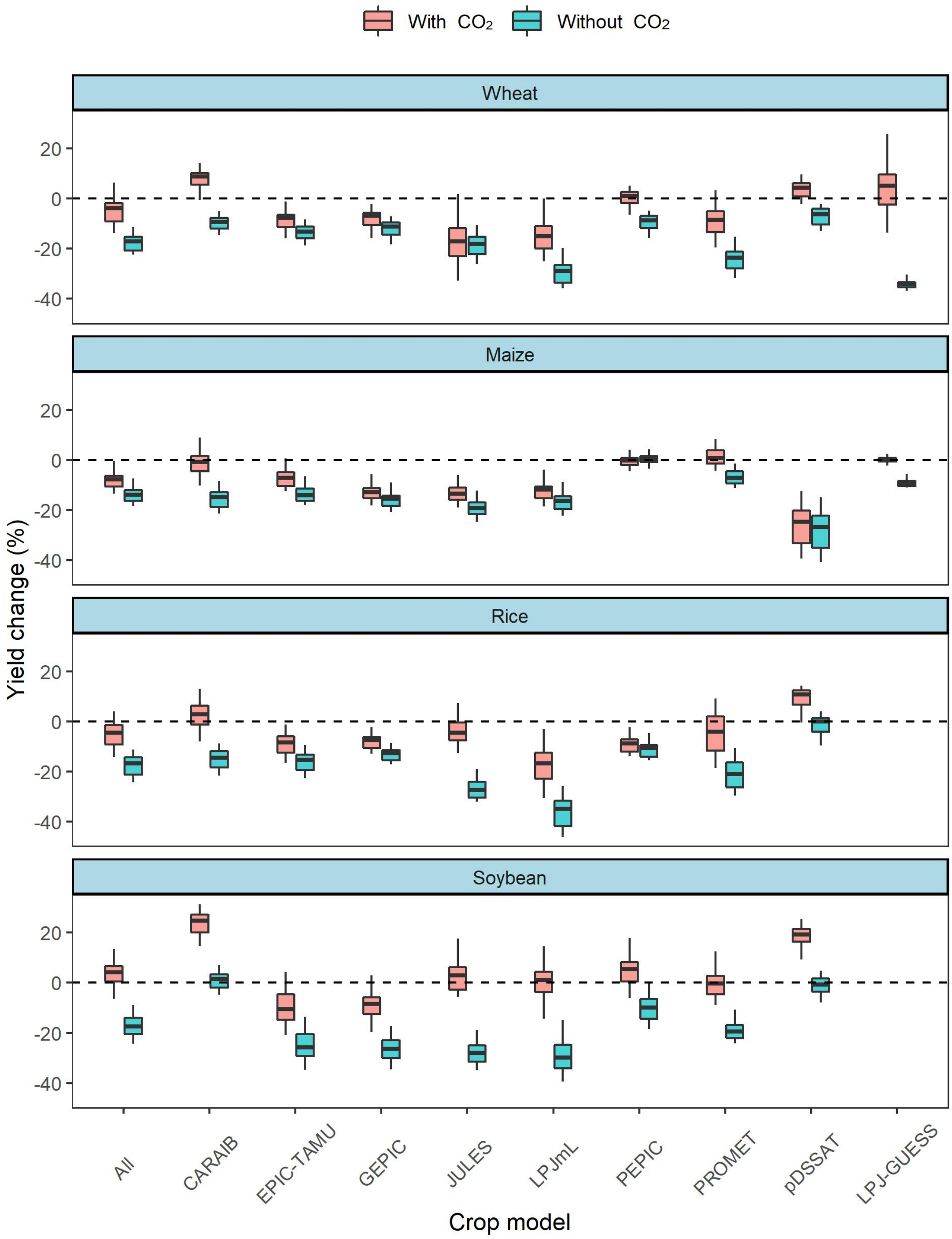

Figure S1 Crop yield change projected by multiple GGCMs and GCMs (9 GGCMs and 32 GCMs) under SSP585 in 2069-2099 compared to baseline (1980-2010). With CO_2 shows projected crop yield with the CO_2 fertilization effect; without CO_2 is projected crop yield without the CO_2 fertilization effect. Box boundaries indicate the 25th and 75th percentiles of crop yields, and whiskers below and above the box indicate the 10th and 90th percentiles. The black lines within each box indicate the median value. Data from the LPJ-GUESS CCGM are not available for rice and soybean.

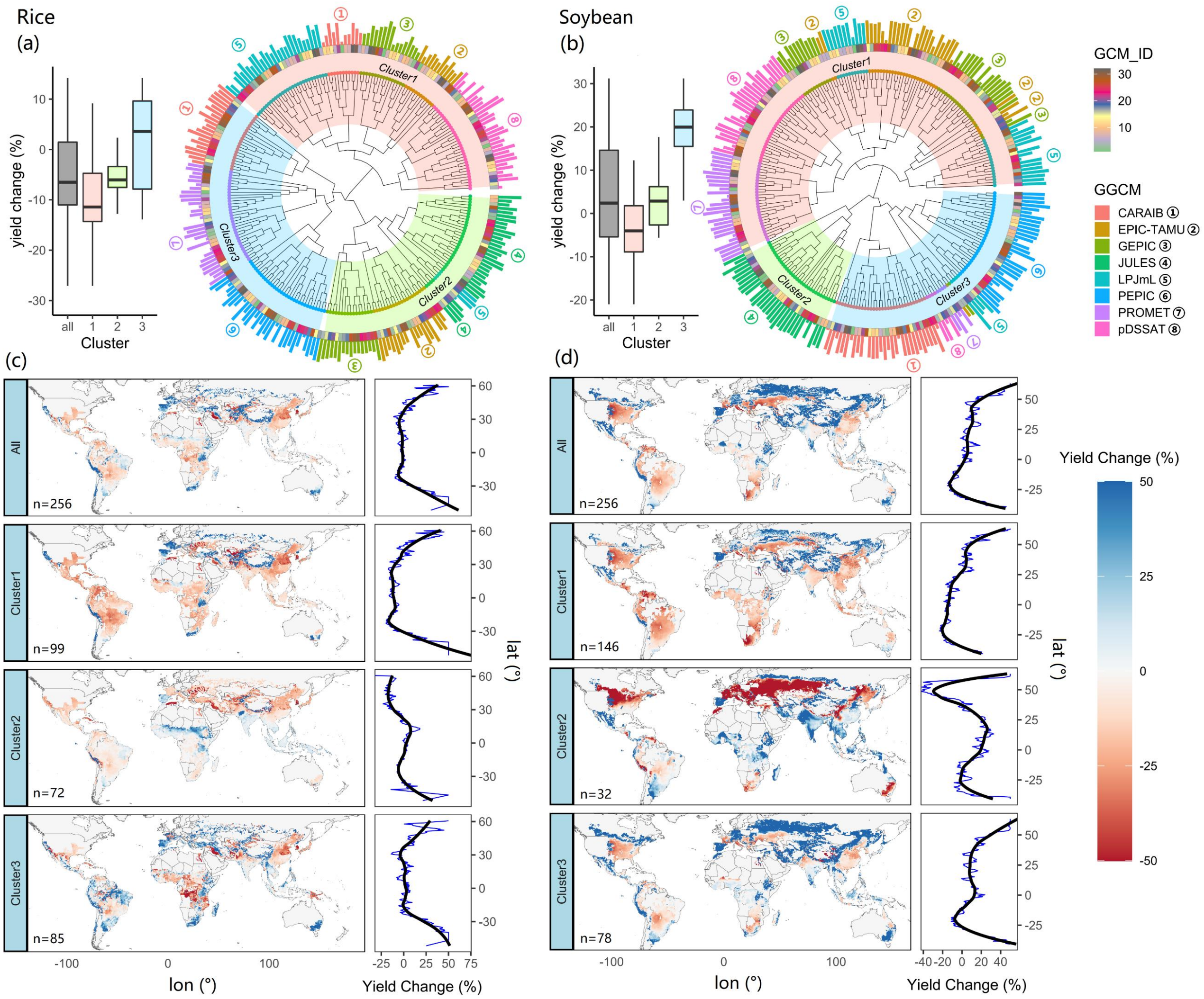

Figure S2 Same as Figure 1 in the main text but for rice and soybean.

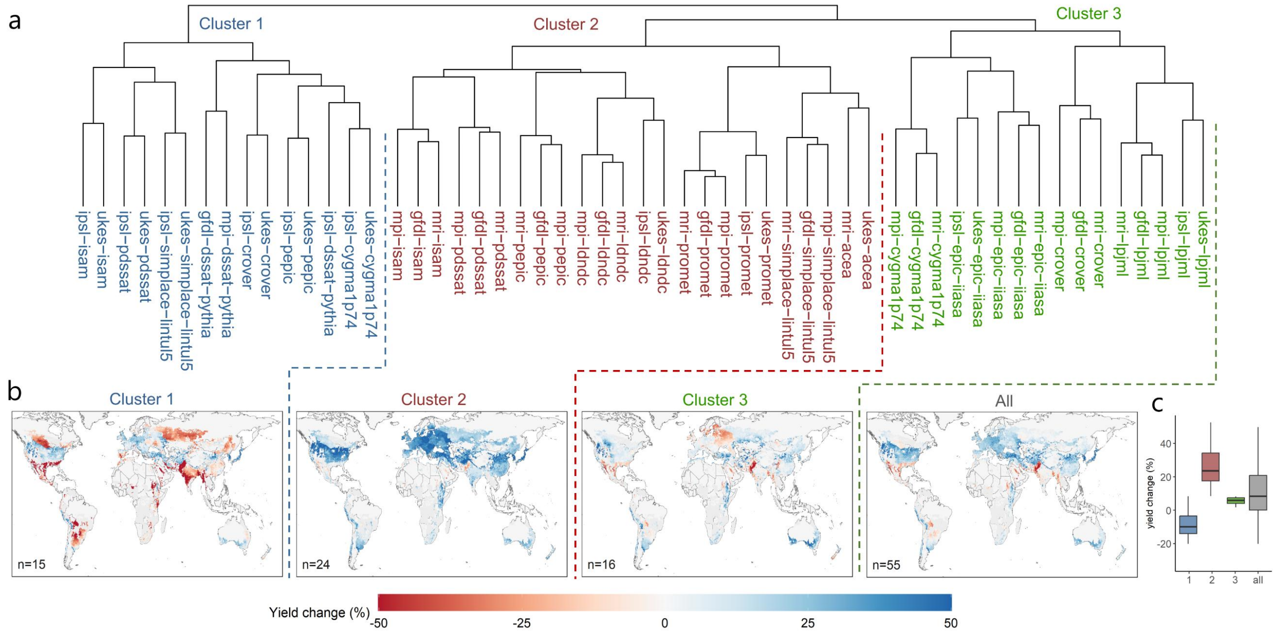

Figure S3 Hierarchical clustering of wheat yield changes (between 2069–2099 and 1980–2010) under SSP585. **a** is the cluster tree diagrams of wheat yield change. The three clusters are highlighted with light red, green, and blue. **b** is the average wheat yield changes for each cluster. The numbers (n=) at the bottom left of each panel represent the number of ensemble members (GGCM×GCM) used for each cluster. **c** is the boxplot showing the change in global yield for each cluster and all models. Box boundaries indicate the 25th and 75th percentiles of crop yield change. The black line within each box indicates the median value. gfdl, GFDL-ESM4; ipsl, IPSL-CM6A-LR; mpi, MPI-ESM1-2-HR; mri, MRI-ESM2-0; ukes, UKESM1-0-LL.

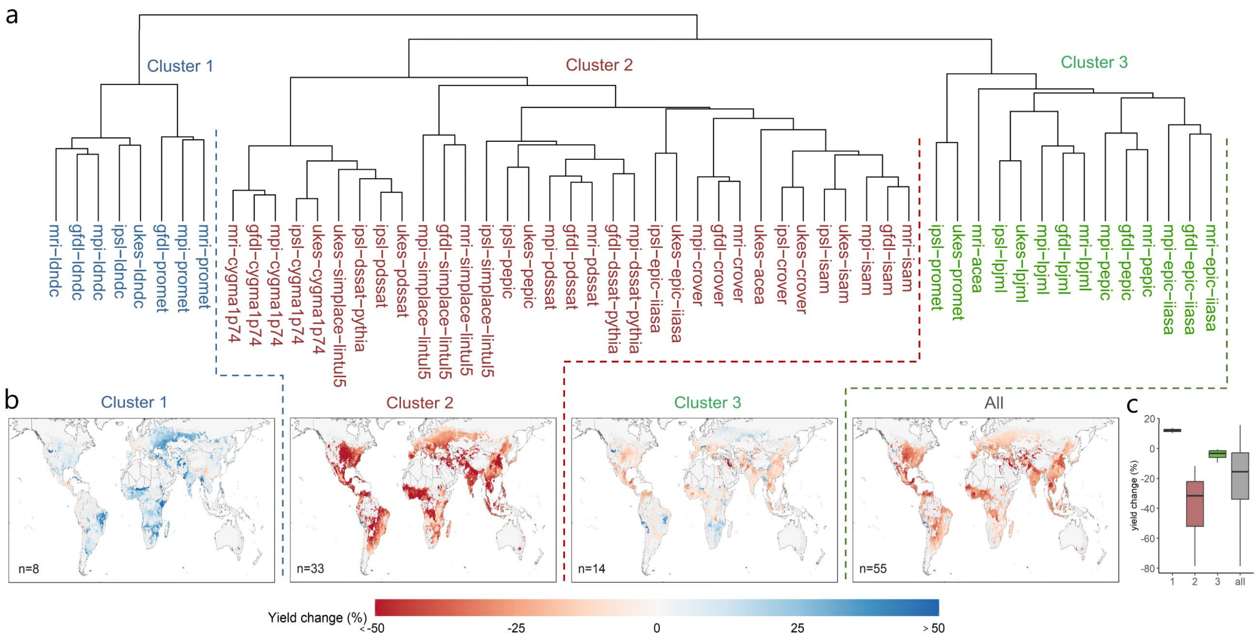

Figure S4 Same as Figure S3 but for maize.

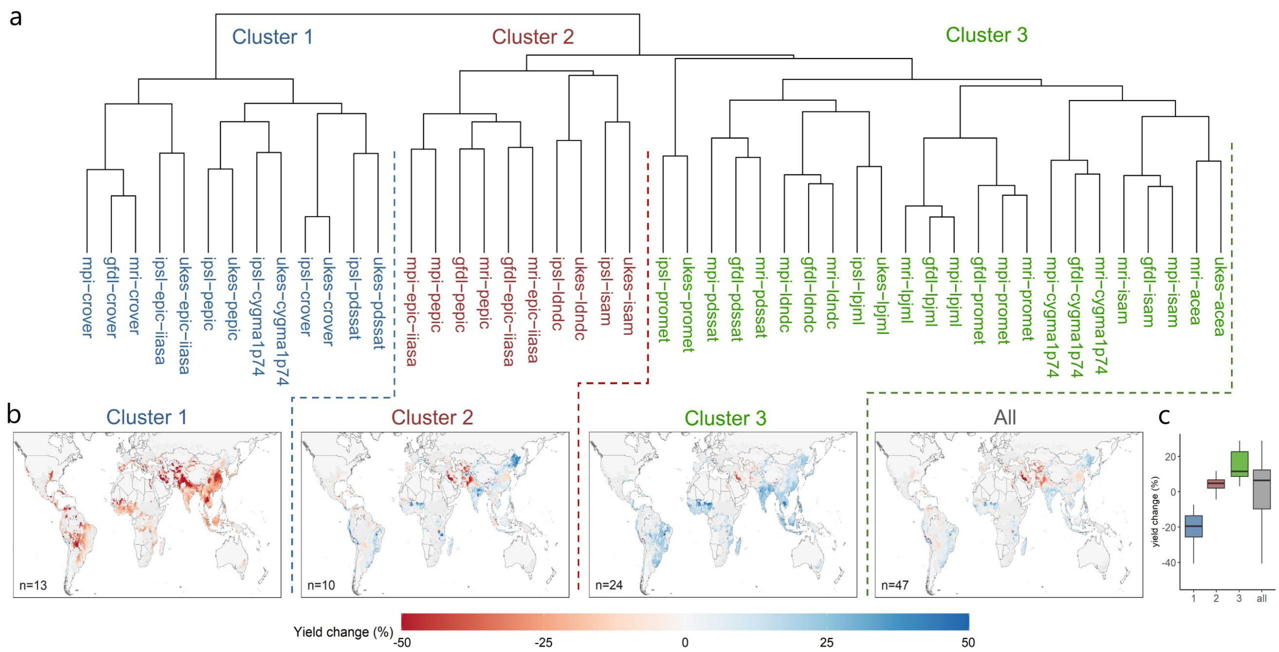

Figure S5 Same as Figure S3 but for rice.

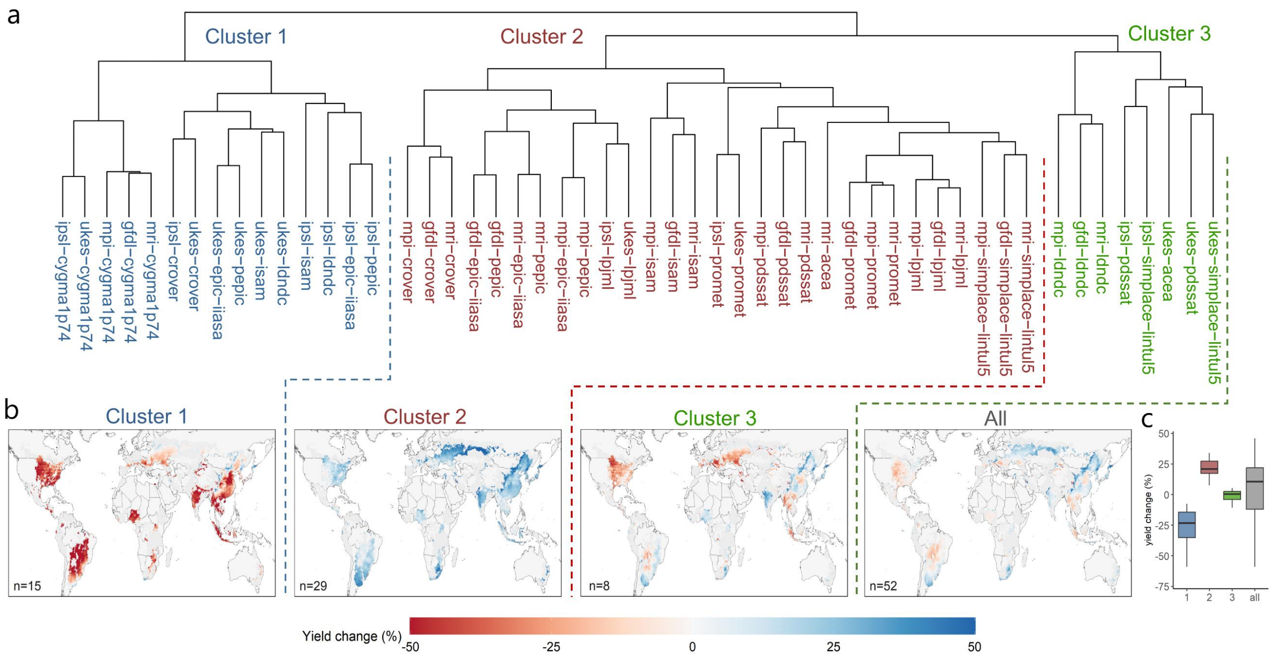

Figure S6 Same as Figure S3 but for soybean.

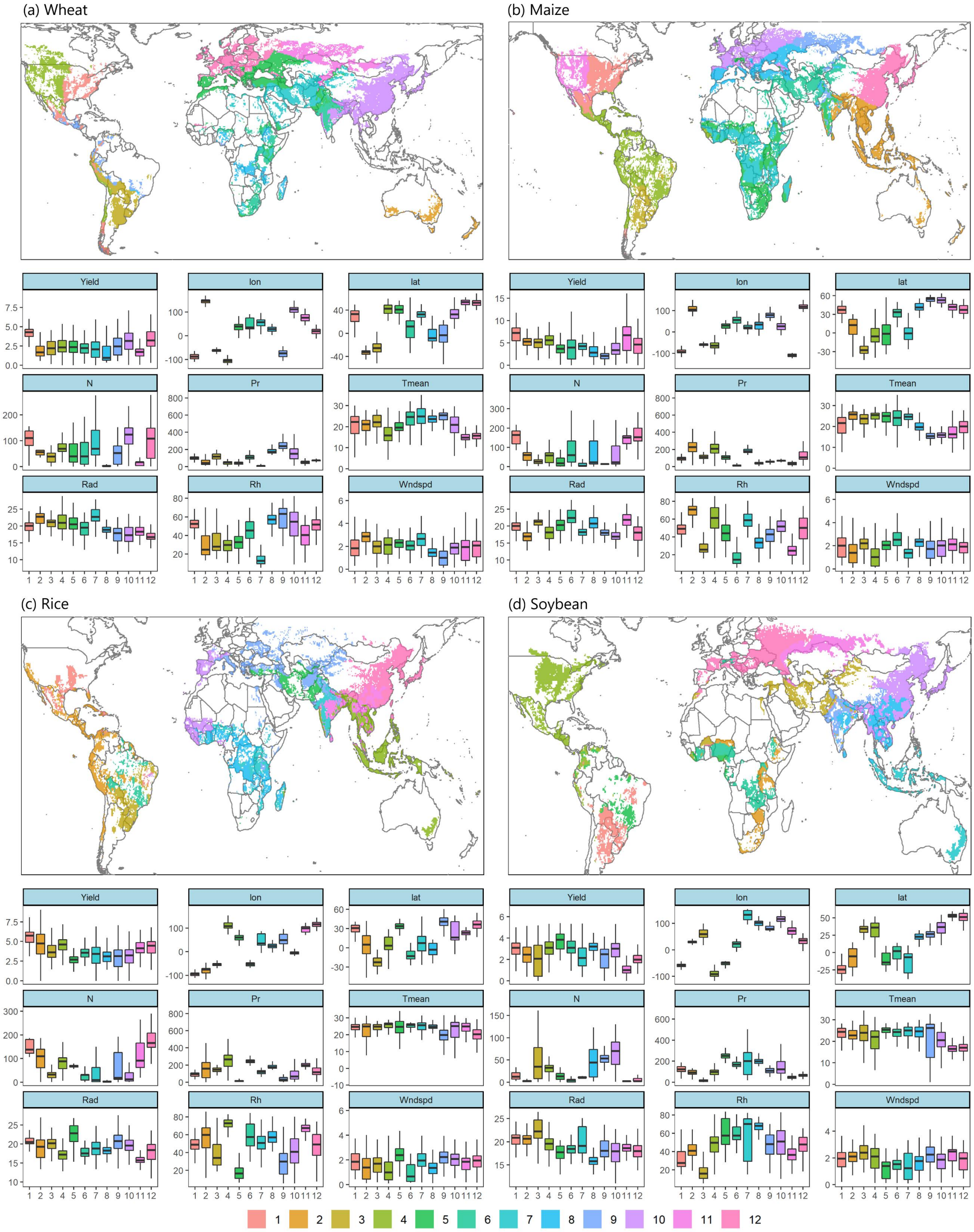

Figure S7 Spatial patterns of cluster divisions (top) based on different variables and the range of different variables (boxplots on the bottom) for wheat (**a**), maize (**b**), rice (**c**), and soybean (**d**). Yield, crop yield (kg/ha); lon, longitude (°); lat, latitude (°); N, nitrogen application rate (kg/ha); Pr, precipitation (mm); Tmean, temperature (°C), Rad, radiation (MJ m^{-2}); RH, relative humidity (%); Wndspd, wind speed (m/s). The k-means clustering was used to produce twelve sub-regions (numbered 1–12, different colors). Box boundaries indicate the 25th and 75th percentiles of each variable, whiskers below and above the box indicate the 10th and 90th percentiles. The black line within each box indicates the median value.

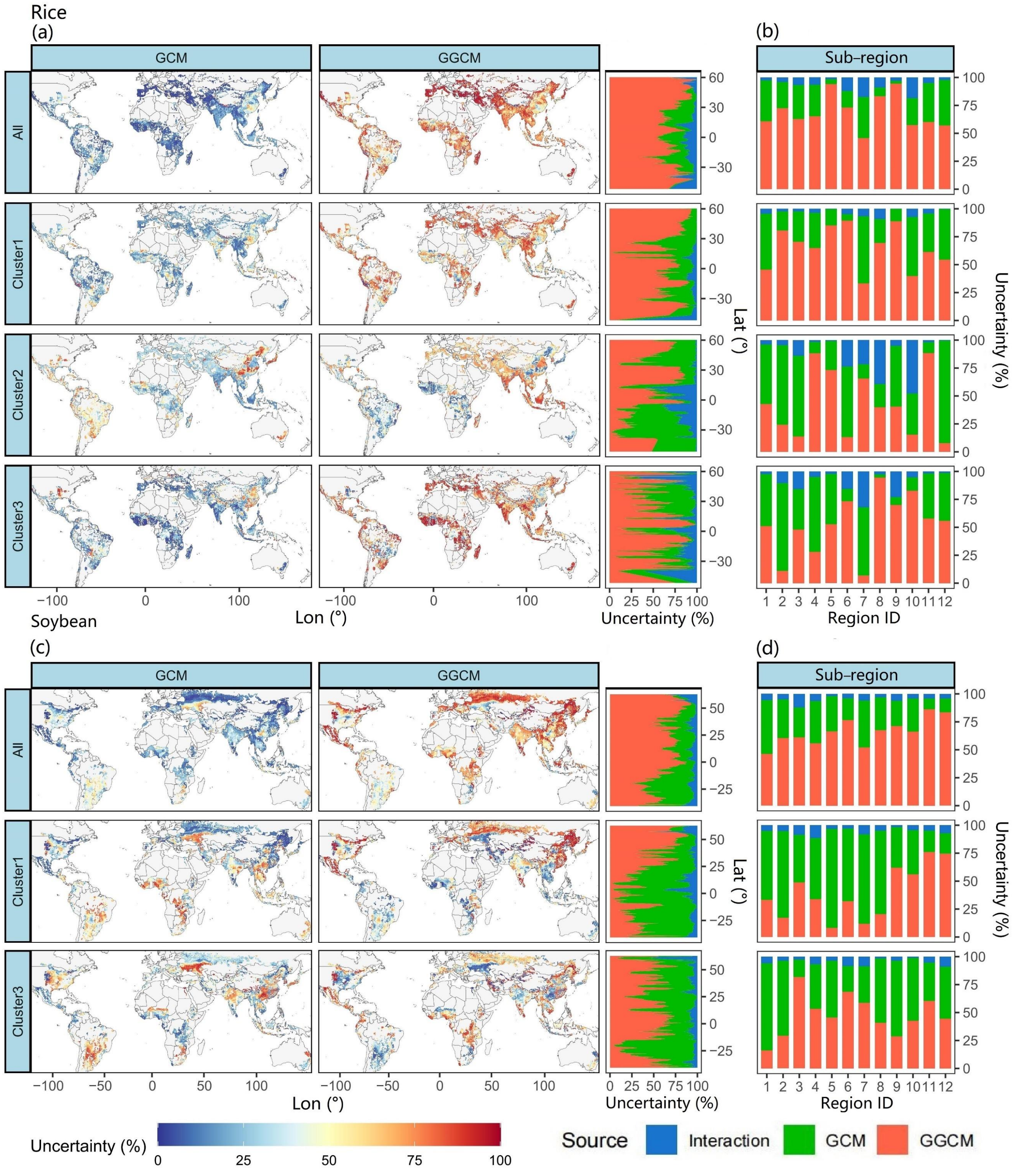

Figure S8 Same as Figure 2 in the main text but for rice and soybean. Since the cluster 2 of soybean only has one GGCM, the uncertainty for cluster 2 is not quantified.

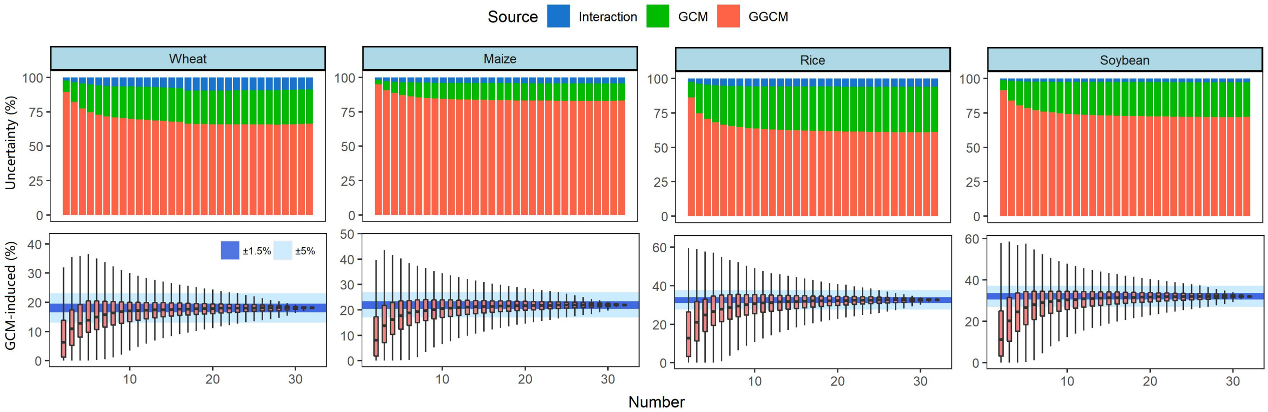

Figure S9 The change of proportion of uncertainty of yield changes in 2069-2099 under SSP585 compared to 1980-2010 with the number of GCMs used for wheat, maize, rice, and soybean. The proportion of uncertainty under each number of GCMs is calculated as all the possible combinations (top panels). The boxplot shows the distribution of uncertainty due to GCM under different numbers of GGCMs used. The dark and light blue shaded areas respectively represent the thresholds of uncertainty of ±1.5% and ±5% when using the contribution of uncertainty estimated from all GCMs as the benchmark. Box boundaries indicate the 25th and 75th percentiles, and whiskers below and above the box indicate the 10th and 90th percentiles. The black lines within each box indicate the median value.

Figure S10 The distribution of uncertainty due to GGCM under different numbers of GGCMs used. The dark and light blue shaded areas respectively represent the thresholds of ±2.5% and ±5% when using the contribution of uncertainty estimated from all GGCMs as the benchmark. Box boundaries indicate the 25th and 75th percentiles. The black lines within each box indicate the median value.

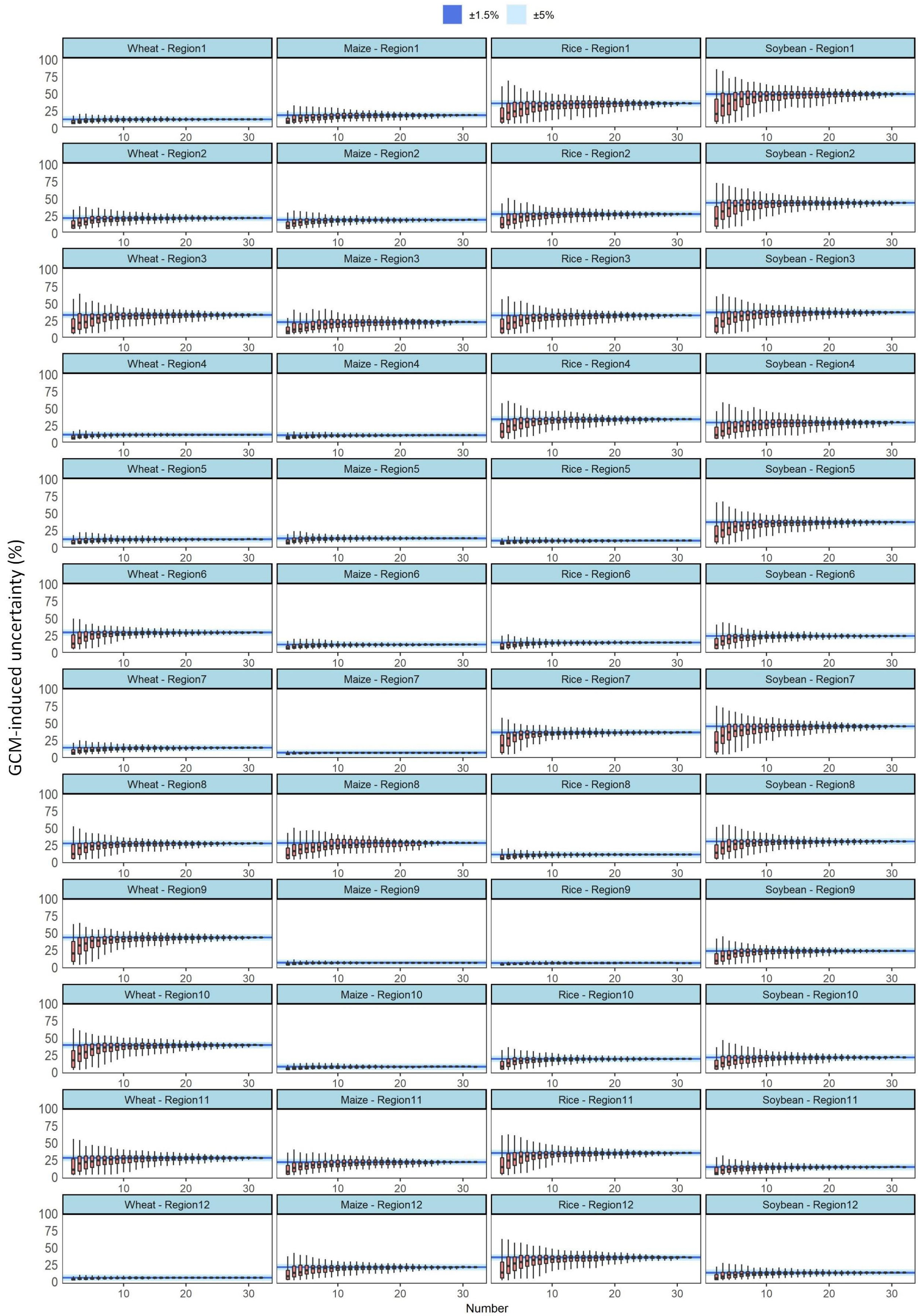

Figure S11 Same as Figure S10 but for GCMs.

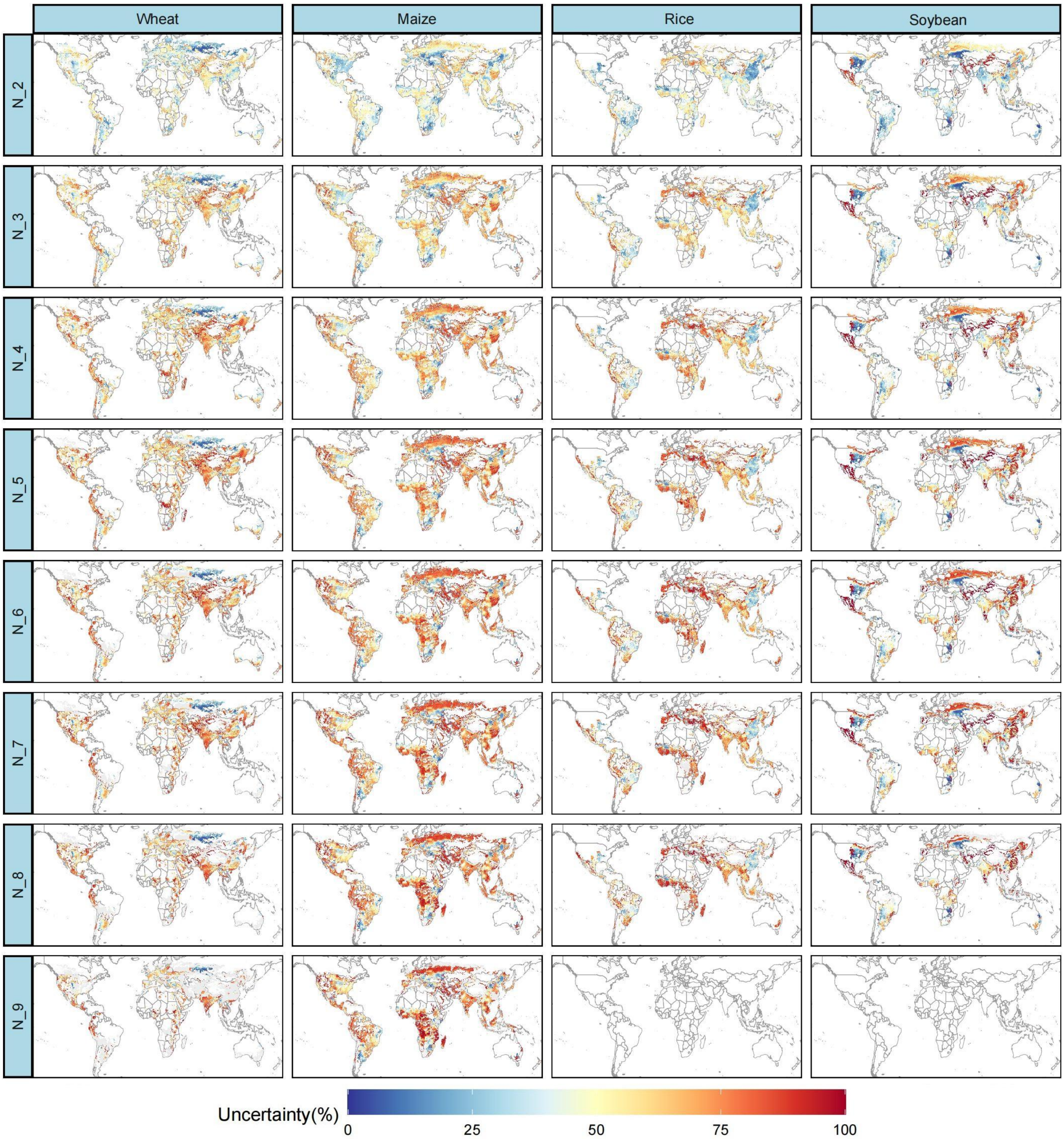

Figure S12 Spatial patterns of GGCM-induced crop yield uncertainty under combinations of different numbers of GGCMs. N_2-N_9 represent the number of GGCMs (from 2 to 9). No data for N_9 as there are 8 GGCMs available for rice and soybean.

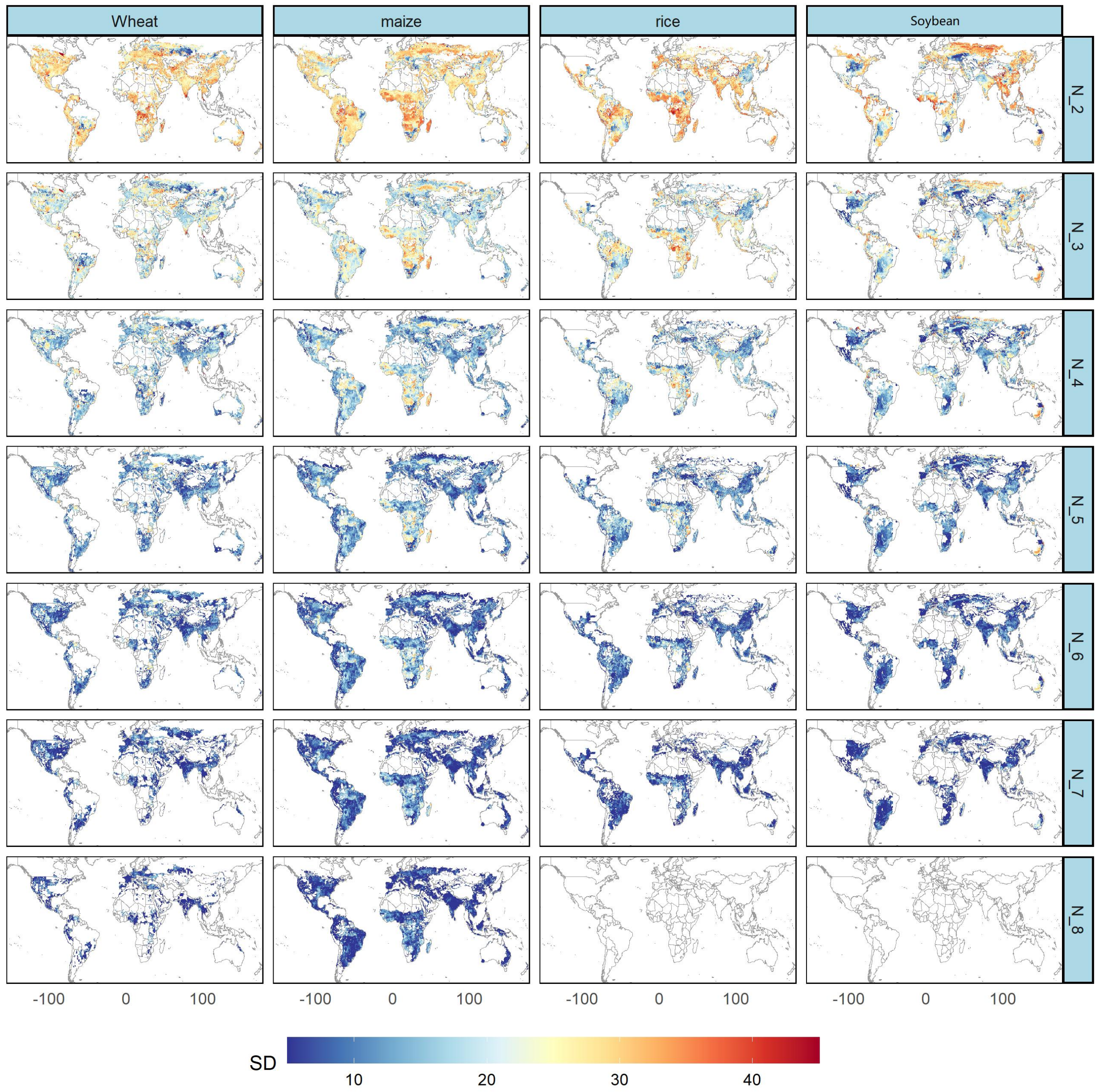

Figure S13 The standard deviation (SD) of GGCM-induced crop yield uncertainty when different numbers of GCMs are used. For example, N_2 is two GCMs are randomly selected from 9 (wheat and maize) or 8 (rice and soybean) GGCMs.

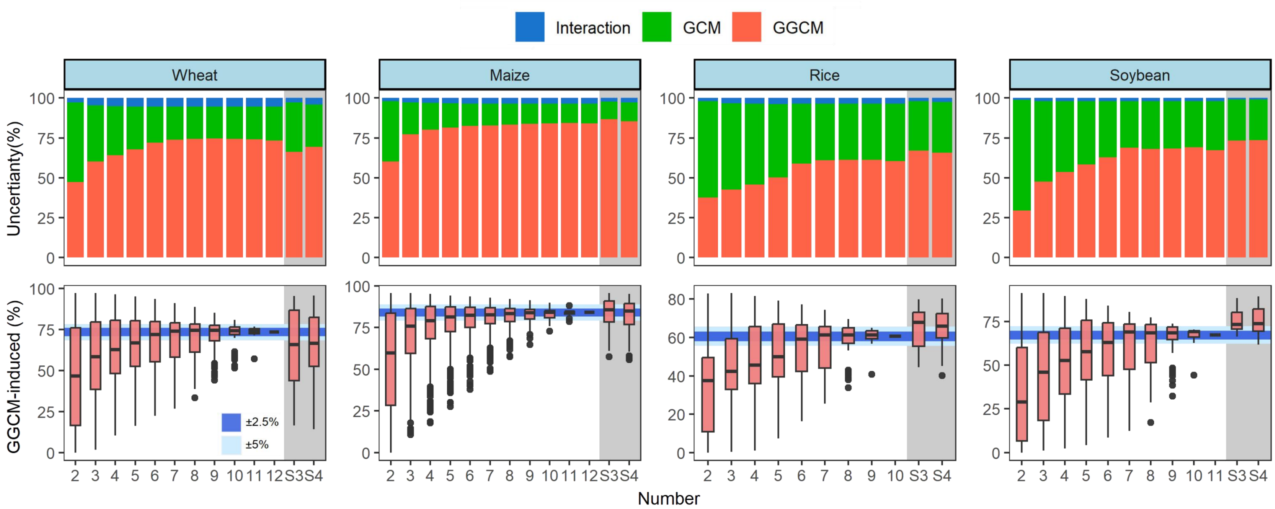

Figure S14 Same as Figure 4 in the main text but for GGCMI phase 3 data.

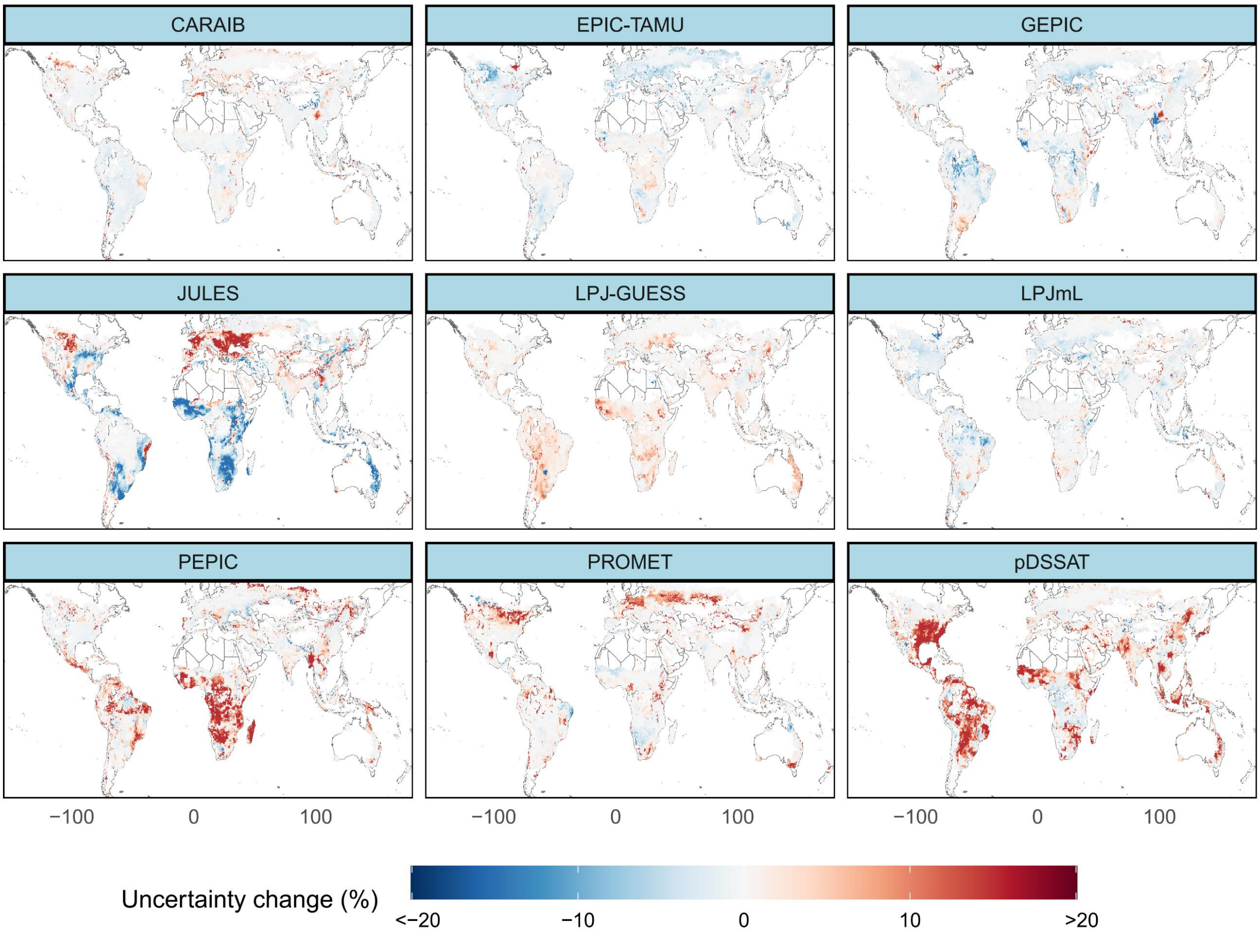

Figure S15 Same as Figure 4 in the main text but for maize.

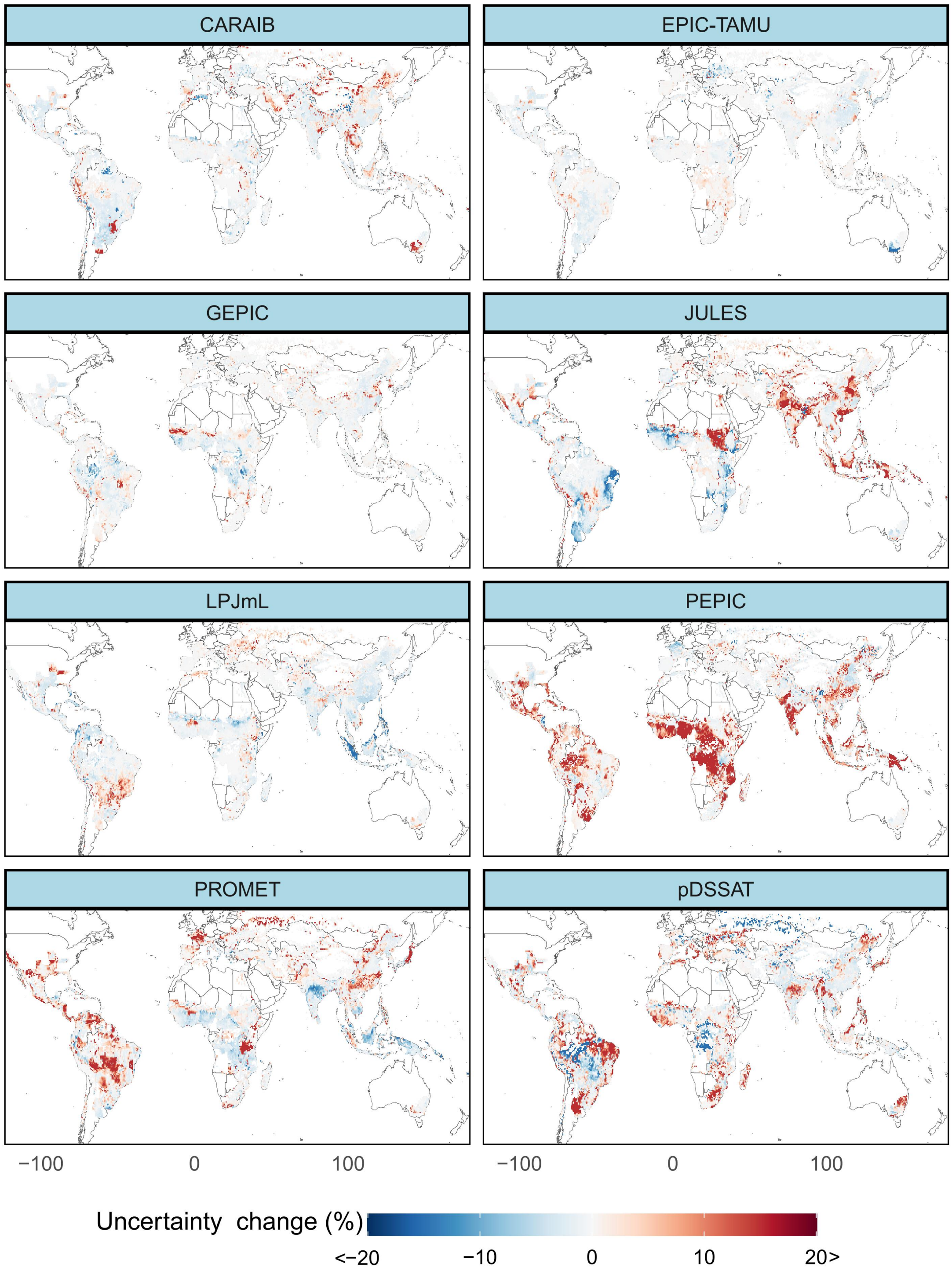

Figure S16 Same as Figure 4 in the main text but for rice.

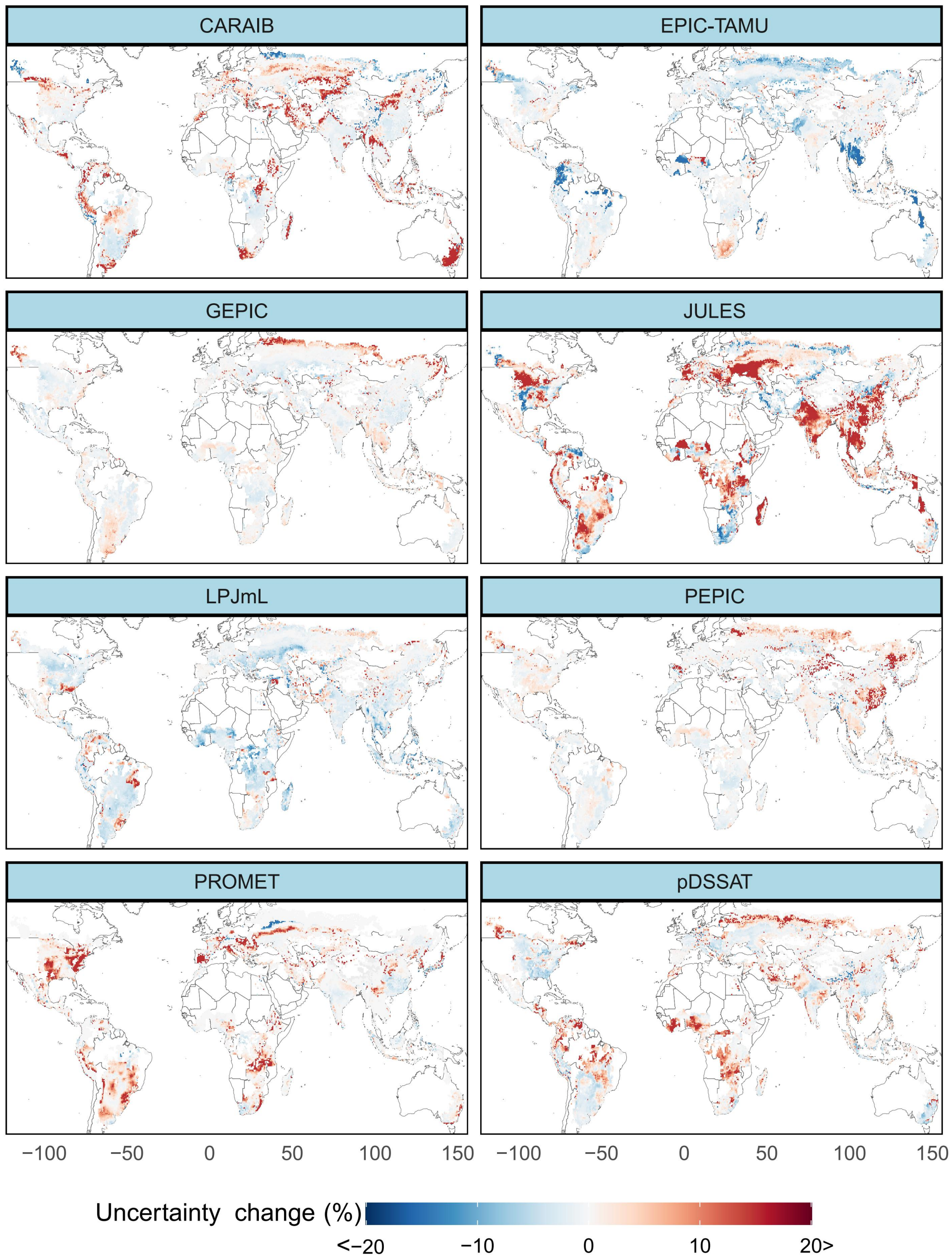

Figure S17 Same as Figure 4 in the main text but for soybean.

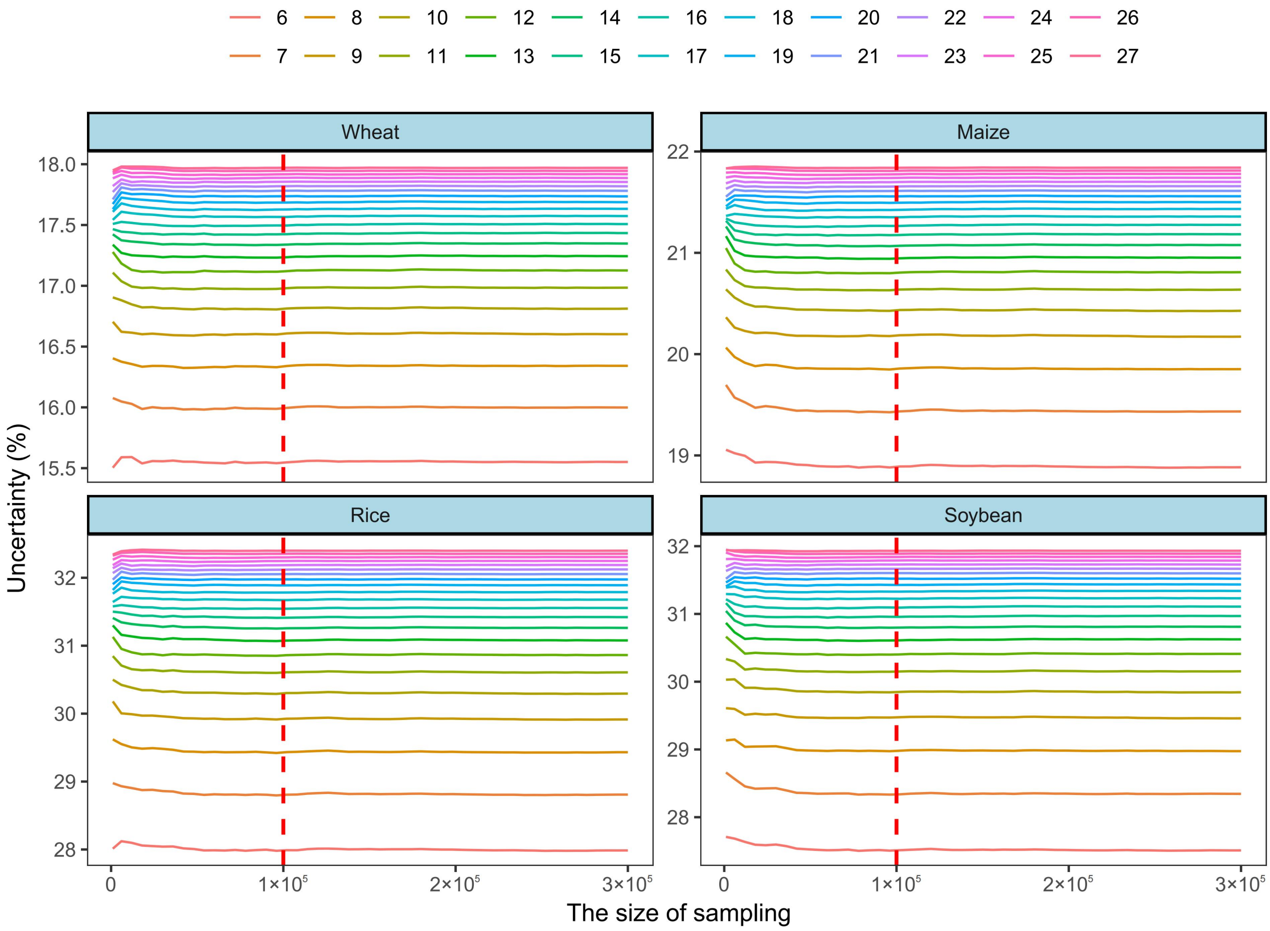

Figure S18 The GCM-induced uncertainty against the size of randomly sampling for wheat, maize, rice, and soybean respectively. The size of randomly sampling under different number of GCMs (from 6 to 27) is from 1000 to 300, 000 for the purpose of demonstration. We finally used 100, 000 as the maximum size of subsampling GCM under 6 to 27 given that uncertainty due to GCM becomes stable when the size approaching to that number.

Table S1 List of 32 global climate models used in this study.

ID	Name of GCM	Institute ID	Resolution (°×°)	ID	Name of GCM	Institute ID	Resolution (°×°)
1	ACCESS-CM2	CSIRO	1.25 × 1.87	17	GFDL-ESM4	NOAA-GFDL	1.0 × 1.3
2	ACCESS-ESM-5	CSIRO	1.25 × 1.88	18	GISS-E2-1-G	NASA-GISS	1.0 × 1.3
3	BCC-CSM2-MR	BCC	1.12 × 1.12	19	INM-CM4-8	INM	1.5 × 2.0
4	CAMS-CSMI-O	CAMS	1.12 × 1.12	20	INM-CM5-0	INM	1.5 × 2.0
5	CanESM5	CCCma	2.8 1× 2.81	21	KACE-1-0-G	NIMS-KMA	1.87 × 1.25
6	CAS-ESM2	CAS	1.4 × 1.4	22	MCM-UA-1-0	UA	3.75 × 2.23
7	CESM2-WACCM	NCAR	0.95 × 1.25	23	MIROC-ES2L	MIROC	2.7 × 2.8
8	CM6A-LR	IPSL	2.5 × 1.3	24	MIROC6	MIROC	1.4 × 1.4
9	CMCC-CMI-SR5	CMCC	0.9 × 1.3	25	MPI-ESM1-2-LR	MPI-M	1.87 × 1.86
10	CMCC-ESM2	CMCC	0.9 × 1.3	26	MPI-ESM1-2-HR	MPI-M	0.94 × 0.94
11	CNRM-CM6-1	CNRM-CERFACS	1.4 × 1.4	27	MRI-ESM2-0	MRI	1.125 × 1.125
12	CNRM-CM6-1-HR	CNRM-CERFACS	1.4 × 1.4	28	NESM3	NUIST	1.87 × 1.87
13	CNRM-ESM2-1	CNRM-CERFACS	1.4 × 1.4	29	NorESM2-LM	NCC	2.5 × 1.9
14	FGOALS-f3-L	CAS	1 × 1	30	NorESM2-MM	NCC	2.5 × 1.9
15	FGOALS-g3	CAS	2 × 2	31	TaiESM1	AS-RCEC	0.9 × 1.25
16	FIO-ESM-2-0	FIO-QLNM	1.25 × 0.9	32	UKESM1-0-LL	UKESM	1.3 × 1.9

Table S2 The variables used in the cluster analysis for dividing sub-regions for four crops.

Type	Variable	Source
Crop	Crop yield (kg/ha)	Multi-GGCMs ensemble mean (1980-2010).
Location	Latitude (°)	The latitude and longitude of each grid.
	Longitude (°)	
Management	N fertilizer input (kg/ha)	Elliott et al. (2015)
Climate	Mean temperature (°C)	https://data.giss.nasa.gov/impacts/agmipcf/agmerra/
	Precipitation (mm)	
	Solar radiation (MJ m^{-2})	
	Relative air humidity (%)	
	Wind speed (m/s)	

Table S3 The minimum effective number of GGCM in uncertainty analysis at global and regional scales.

Regions	Wheat	Maize	Rice	Soybean
Global	6	6	6	5
Sub-region 1	3	5	5	5
Sub-region 2	5	6	5	5
Sub-region 3	6	6	6	6
Sub-region 4	4	5	3	5
Sub-region 5	4	5	5	4
Sub-region 6	5	5	6	4
Sub-region 7	5	5	5	5
Sub-region 8	6	6	5	5
Sub-region 9	6	3	4	4
Sub-region 10	8	4	5	5
Sub-region 11	6	5	3	4
Sub-region 12	3	6	5	5

Table S4 The minimum effective number of GCM in uncertainty analysis at global and regional scales.

Regions	Wheat	Maize	Rice	Soybean
Global	9	10	12	12
Sub-region 1	6	11	14	13
Sub-region 2	10	8	11	12
Sub-region 3	12	13	14	13
Sub-region 4	5	6	13	13
Sub-region 5	6	6	6	13
Sub-region 6	10	6	7	10
Sub-region 7	8	3	11	13
Sub-region 8	11	15	6	12
Sub-region 9	13	3	4	10
Sub-region 10	12	6	9	7
Sub-region 11	11	13	13	6
Sub-region 12	4	7	12	7